Antimicrobial Effect of *Azadirachta indica*, *gum* Stabilized Cobalt Doped ZnO Nanoparticles

A. GEETHA[1], BA. ANANDH[2]* and R. SAKTHIVEL[2]

[1]Department of Chemistry, Hindusthan College of Arts and Science, Coimbatore, India.
[2]Department of Electronics, PSG College of Arts & Science, Coimbatore, India.
*Corresponding author E-mail: anandh.ba@gmail.com

ABSTRACT

The wet chemical approach was used to synthesize the AI-gum stabilized ZnO nanoparticles doped with cobalt. The structural, morphological, antibacterial, and antifungal activity of AI stabilized at various cobalt concentrations were investigated. X-Ray Diffraction (XRD) pattern shows hexagonal form oriented on the c-axis. The presence of a spherical-shaped object has been confirmed using a Field Emission Scanning Electron Microscope (FESEM). Zinc, cobalt and oxygen atom's presence is confirmed by Energy Dispersive X-ray (EDAX). Antibacterial activity on *S. aureus* reveals the maximum inhibition zone compared with the antibacterial activity of *E. coli*. Antifungal activity against *Aspergillus fumigatus* reveals the maximum inhibitory zone in contrast to *Candida albicans*.

Keywords: XRD, FESEM, EDAX, ZnO, Antibacterial and antifungal activity.

INTRODUCTION

ZnO is an II-IV group semiconductor that has a wide bandgap of 3.2 eV at ambient temperature that has been employed in a variety of applications. ZnO is recommended for applications such as optoelectronics[1], Diodes[2], transparent conductive oxide[3], gas sensors[4], biosensors[5], and antibacterial agents[6] due to its low cost, abundance, and environmental friendliness. Currently, efforts are being taken to enhance the ZnO nanostructure's properties by doping them with several metal oxides such as In[7], Mn[8], Sn[9], Al[10,11], Bi[12], Ga[13] and Mg[14]. Cobalt, one of the dopants, has proven to be particularly useful in modifying the electronic structure. Owing to transition among Co 3d ligands field split levels and filled 3d electron shells of Zn^{2+}, the replacement Co^{2+} with Zn^{2+} tetrahedra ligand-coordinated (Td) sites in the ZnO lattice makes a significant increase in the absorption peaks at the visual spectrum[15]. These changes make charge imbalance and increase the antimicrobial activity of Cobalt doped ZnO nanoparticles by inducing photoconductivity[16]. As a result, cobalt is chosen for doping into ZnO to improve antibacterial characteristics.

MATERIALS AND METHODS

Chemicals with a purity of 99.9% were

obtained from Sigma-Aldrich Germany were used in this study. Sodium hydroxide, Zinc nitrate, and stabilizing agent (*Azadirachta indica gum*) were used to make Co:ZnO nanoparticles. Double distilled water was utilized as a solvent.

Synthesis of Co:ZnO Nanoparticles

Botanical Survey of India (BSI), Coimbatore validated the *Azadirachta indica gum* exudates which were obtained at the PSG College of Arts & Science. *Azadirachta indica gum* exudation was rinsed in purified water to eliminate contaminants. The gum was completely dissolved in the solvent and Whatman filter paper was used for filtering to obtain a glassy lump of pure gum.

A simple wet chemical approach was used to make high purity metal-doped ZnO nanoparticles. In 90 mL of double-distilled water, 1 g zinc nitrate was dissolved. After 10 min of stirring, 100 mg of AI gum was mixed with 10 mL of water. Cobalt nitrate with 0.03, 0.05, and 0.07 concentrations were mixed with the solution. The NaOH solution (100 mL) is then added, drop by drop, for 3 h with vigorous shaking. Centrifugation of the suspension was done and a hot air oven at 100°C was used to dry the nanoparticles. Co:ZnO nanoparticles were produced as a light green crystalline powder.

Antibacterial assay

The antibacterial action of cobalt doped ZnO nanoparticles stabilized with AI gum was tested using the agar well diffusion method. *Staphylococcus aureus (S. aureus)* and *Escherichia coli (E. coli)* bacteria were used in this research. The Muller Hinton agar was sterilised and prepared. The agar surface was swabbed with the test specimens by a sterile cotton swab. On the agar medium, wells have been formed with the help of sterilized gel puncture. 10 µL of the sample was poured into the created wells and 24 h of incubation of these dishes were done at 37˚C. The clear zones were used to assess the efficiency of the samples.

Antifungal assay

The antifungal test activity was done using the Well diffusion method for the provided sample on several fungal strains. The fungicidal impact of the provided sample was determined by the inhibition of the fungus's mycelial growth, which was noted as an inhibition zone close to the wells.

The antifungal activity of plant extracts was tested using *Candida albicans* and *Aspergillus fumigatus* acquired from PSG Institute of Medical Sciences & Research Hospital. The Petri plates were coated with potato dextrose agar, which had been prepared and sterilised. Using a sterile cotton swab, testing fungal cultures have been scrubbed over the agar medium on every plate. With the help of sterile gel puncture, wells were made on the surface of the agar, and around 100 µL of the provided samples were loaded into the wells. After three days of incubation at room temperature, the antifungal impact was visible as a crescent inhibitory zone.

RESULTS AND DISCUSSION

XRD Analysis

XRD patterns for Co-doped (0.03, 0.05 and 0.07) ZnO nanoparticles are shown in Fig. 1. The clear and strong peaks in XRD of the samples disclose that they are highly pure and crystalline. The ZnO has a hexagonal wurtzite structure which is confirmed by the strong diffraction pattern at (100), (002) and (101). The peaks that appeared in the XRD waveform are near match with 36-1451 standard JCPDS Card. The XRD findings show that there are no further peaks associated with cobalt metal or any other oxide phase which confirms the prepared samples are of a single-phase nature.
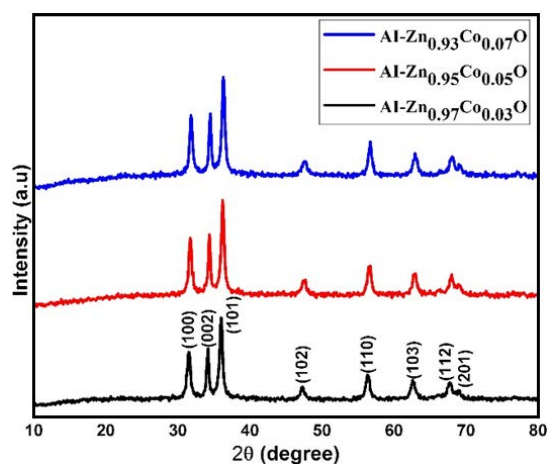

Fig. 1. XRD spectra of Co:ZnO nanoparticles stabilized with AI gum

Table 1 shows the values of strain (ε), dislocation density (δ), and the lattice values 'a' and 'c' of Co:ZnO nanoparticles stabilized with AI gum. These values are close to the standard values of a = 3.251 and c = 5.212. The replacement of Zn^{2+}

ions in the ZnO matrix by Co^{2+} ions could be the reason for the rise in the lattice parameters. The dislocation density and microstrain were found to be increased with an increase in the doping ratio. The variation in ionic radii among Zn (0.74) and Co (0.78), as well as the presence of Co^{2+} in an octahedral atmosphere in the wurtzite structure, could explain the shift in the lattice parameter value. Hence, the XRD pattern shifts, which attributes to a rise in reductions and lattice strain[17]. The rise in the size of particles confirmed the insertion of cobalt in the ZnO matrix. The existence of Co^{2+} in the interstitial site alters the ratio of intermittent Zn, oxygen, and Zn vacancies.

Table 1: Strain, Dislocation density and Lattice parameters of Co:ZnO nanoparticles stabilized with Al gum

Sl. No	Samples	Strain $(\varepsilon) \times 10^{-3}$	Dislocation density $(\delta) \times 10^{15}$ lines/m^2	Lattice parameters (Å) a	c
1	$Al\text{-}Zn_{0.97}Co_{0.03}O$	2.259	4.2477 E+15	3.2798	5.2518
2	$Al\text{-}Zn_{0.95}Co_{0.05}O$	2.247	4.1133 E+15	3.2580	5.2203
3	$Al\text{-}Zn_{0.93}Co_{0.07}O$	2.223	4.2007 E+15	3.2478	5.2042

The line widening may be due to the rise in the microstrain and crystallite size of nanoparticles. The minor change in 2θ in the diffraction pattern and shrinking of the peak is attributable to a rise in microstrain. The diffraction peak position shows the inclusion of Co^{2+} ions in the ZnO matrix, indicating that there is no visible alteration in the crystal structure as a result of Co doping.

Table 2: Structural values of Co:ZnO nanoparticles stabilized with Al gum

Sl. No	Samples	hkl	Crystal Size (nm)	FWHM	d (A°)	2θ (degree)
1	$Al\text{-}Zn_{0.97}Co_{0.03}O$	100	15	0.5382	2.83	31.48
		002	15	0.5731	2.62	34.13
		101	18	0.4569	2.49	35.97
2	$Al\text{-}Zn_{0.95}Co_{0.05}O$	100	16	0.5299	2.82	31.70
		002	16	0.5197	2.60	34.34
		101	18	0.4535	2.47	36.19
3	$Al\text{-}Zn_{0.93}Co_{0.07}O$	100	16	0.5355	2.81	31.80
		002	16	0.5148	2.60	34.45
		101	19	0.4493	2.47	36.29

Table 2 shows 2θ readings with associated hkl values, obtained FWHM and computed crystallite sizes. Scherrer's formula[18] was used to calculate the crystallite size (D) of the nanoparticles. As the dopant ratio increases from 0.03 to 0.07 g, the crystallite size of cobalt doped ZnO rises from 16 to 19nm. The slight rise in crystallite size could be attributed to cobalt's lower dissolvability in the ZnO lattice.

FTIR Analysis

Fourier Transform Infrared Spectroscopy is the method to disclose details about a material's molecular structure or chemical bonding. This method confirms the interaction between the Al gum and the prepared nanoparticles. The FTIR spectrum at room temperature of Co incorporated ZnO nanoparticles stabilized with Al gum is shown in Fig. 2. The absorption spectrum between 3400 cm^{-1} and 3500 cm^{-1} is caused by the widening of the O-H group. This shows the presence of hydroxyl groups found in Al gum as well as the presence of a small amount of water absorption by the ZnO nanostructure[19].

The >C=O bond is responsible for the peaks at 1620 cm^{-1}, 1632 cm^{-1} and 1647 cm^{-1}. The band in the 400 cm^{-1} -500 cm^{-1} region is related to (ZnO) metal oxide bond[31,32]. In the spectrum of $Al\text{-}Zn_{0.97}Co_{0.03}O$, $Al\text{-}Zn_{0.9}5Co_{0.05}O$, $Al\text{-}Zn_{0.93}Co_{0.07}O$, the frequency of the Zn-O bond is moved to the greater wavelength side. The above shift could be attributed to the substitution of Co (atomic mass = 58.9) for Zn (atomic mass = 65.3). C = N band has no significant change and the C-O band has a larger shift. In the spectrum, no peak associated with cobalt oxide was noticed which implies that Co ions have been replaced in the standard lattice of ZnO.
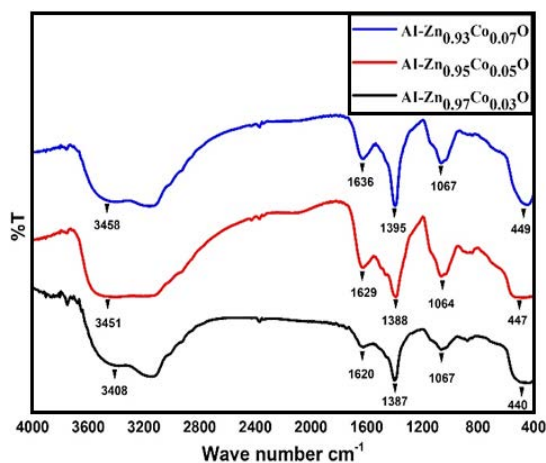
Fig. 2. FTIR Spectrum of Co:ZnO nanoparticles stabilized with Al gum

EDAX and FESEM

EDAX and FESEM analysis were used to identify elemental compositions and morphological properties of Co:ZnO nanoparticles stabilized with Al gum. EDAX study was used to determine the extent of Co incorporation and the content of Co:ZnO nanoparticles stabilized with Al gum and is shown in Fig. 3 with varying Co ratios. The peaks present in the EDAX spectrum confirm the presence of Zn, O, and Co which shows the incorporation of Co^{2+} in the ZnO lattice. The inset in Fig. 3 shows the elemental composition of Co:ZnO nanoparticles. The atomic percentage demonstrates the crystalline phase of the samples.
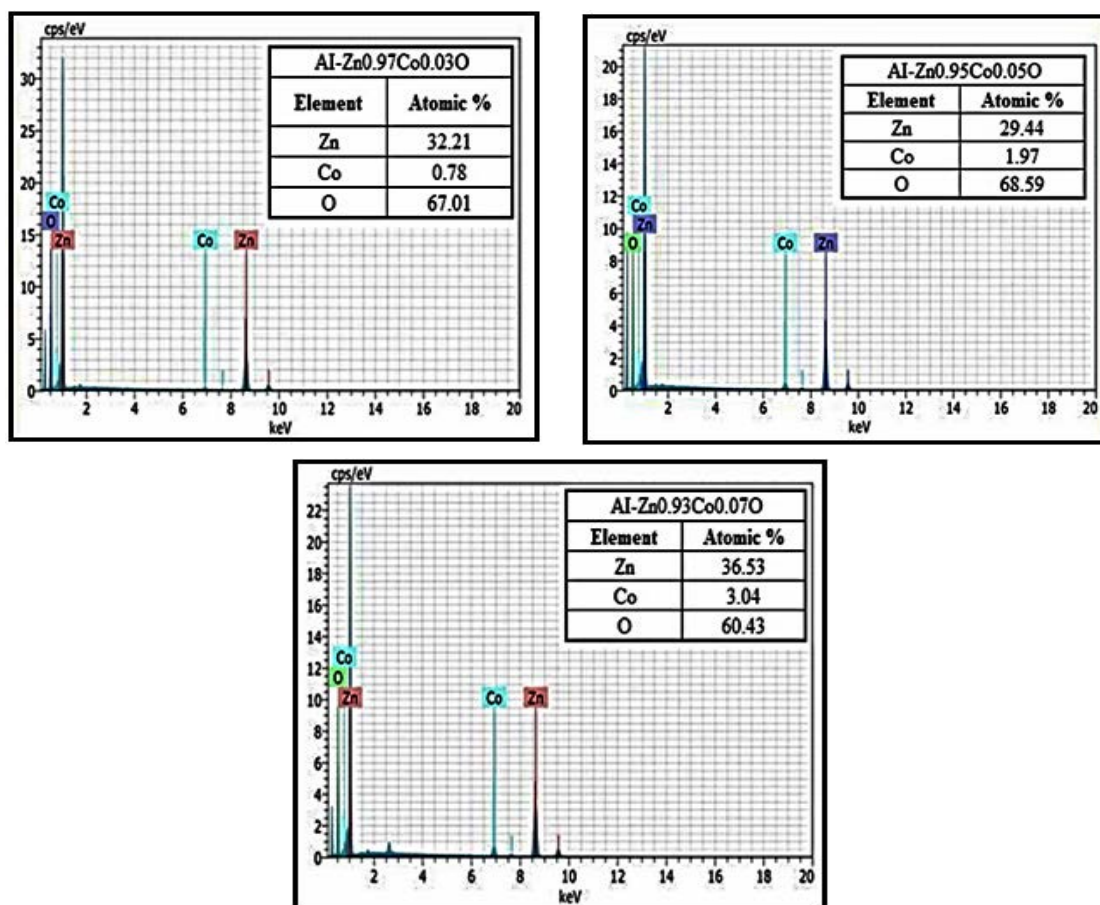

Fig. 3. EDAX spectra of Co:ZnO nanoparticles stabilized with Al gum

FESEM images of Co:ZnO nanoparticles stabilized with Al gum with different Co ratio is shown in Fig. 4. The images clearly show that all the particles are spherical. The increase in the Co dopant ratio in ZnO causes self-agglomeration, which results in a higher size of particles, which was also reflected in the XRD result.
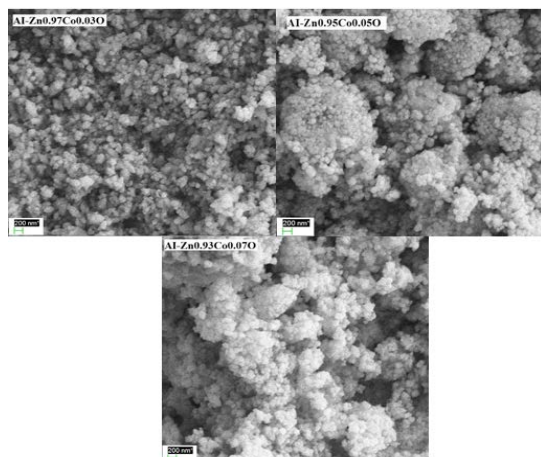
Fig. 4. FESEM images Co:ZnO nanoparticles stabilized with Al gum

UV-Visible Absorption Spectra Analysis

The spectra of UV-Vis absorption shown in Fig. 5 represent the impact of Co^{2+} dopant on the optical characteristics of ZnO nanoparticles. The spectra clearly show that as the Co^{2+} content increases, the absorption peaks shifted slightly to the shorter wavelength side. It is due to a slight rise in crystal size from 16nm to 19nm. The blue shift in the lower wavelength side is also explained by the Quantum confinement effect[20]. The direct transition equation was used to compute the bandgap of Co^{2+} doped ZnO nanoparticles, and the calculated bandgap energies of the $Zn_{0.97}Co_{0.03}O$, $Zn_{0.95}Co_{0.05}O$, and $Zn_{0.93}Co_{0.07}O$ nanoparticles are 3.55eV, 3.57eV, and 3.59eV, respectively[21,22].
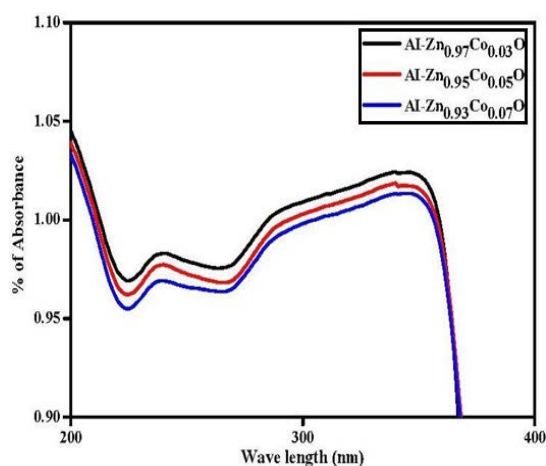

Fig. 5. UV-Vis absorption spectrum of Co:ZnO nanoparticles stabilized with Al gum

Antibacterial applications

Antibacterial assessment of Co:ZnO nanoparticles stabilized with Al gum was carried over the pathogenic *S. aureus (Gram-positive)* and *E. coli (Gram-negative)* bacteria. To assess antibacterial efficacy against pathogenic organisms, well diffusion assessment was performed over Nutrient agar. Fig. 6 and 7 depict antibacterial plates and the maximum zone of inhibition graph of *E. coli* and *S. aureus* bacteria.

The antibacterial activity of the Al-ZnO increases as the Co doping ratio increases. The rough surface layer of ZnO, which is created by the Co dopant, also helps to improve its antibacterial action[23]. The antibacterial action of ZnO has previously been attributed to the generation of reactive oxygen species, the release of Zn^{2+} ions, and cell layer instability[24]. The Al gum stabilized ZnO with 7% Co doping has the best antibacterial action against *S. aureus*. Snega *et al.,*[25] explored why *Gram-positive* bacteria had more antibacterial activity than *Gram-negative* bacteria. Negatively charged radicals quickly adhere to *Gram-positive* bacteria's cell membrane, thus killing the bacterium.
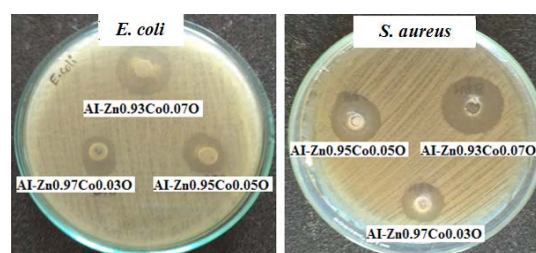

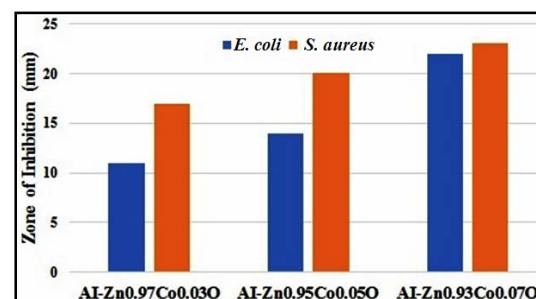**Fig. 6. Antibacterial plates of Co:ZnO nanoparticles stabilized with Al gum**

Fig. 7. Antibacterial Maximum Zone of Inhibition of Co:ZnO stabilized with Al gum

Antifungal applications

Figures 8 and 9 depict the antifungal plates and the corresponding maximum zone of inhibition graph of the fungal pathogens, *Candida albicans* and *Aspergillus fumigatus*. Metal ions generated from the doped nanoparticle

might affect antifungal action by breaking the cell membrane and obtaining access[26]. AI-$Zn_{0.93}Co_{0.07}O$ shows maximum inhibition zone and AI-$Zn_{0.97}Co_{0.03}O$, $Zn_{0.95}Co_{0.05}O$ show lesser activity. The findings show that ZnO nanoparticles can prevent food poisoning, allergies and water
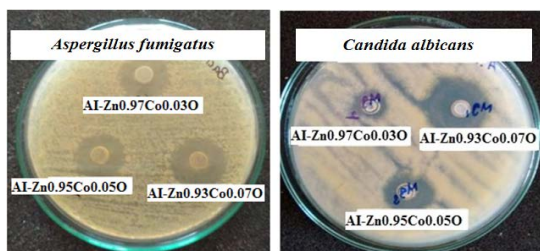

Fig. 8. Antifungal plates of Co:ZnO nanoparticles stabilized with AI gum

CONCLUSION

In conclusion, the wet chemical method was used to synthesize Co:ZnO hexagonal nanoparticles stabilized with AI-gum for different Co ratios. The addition of Co dopant does not affect the crystal lattice or morphologies of ZnO, but it has increased the average particle size, as confirmed by XRD and FESEM data. Co doping can boost the antibacterial

adulteration, as well as act as drug-resistant pneumonia. As a result, Co:ZnO nanoparticles stabilized with AI gum are employed in pharma for creating the finest drug for pneumonia.
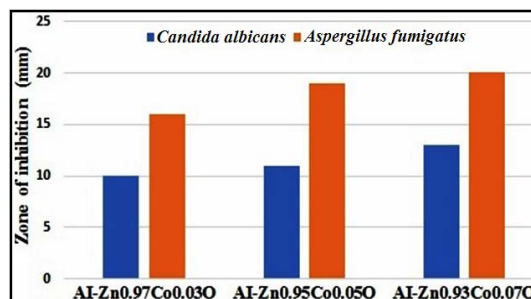

Fig. 9. Antifungal Maximum Zone of Inhibition of Co:ZnO stabilized with AI gum

activity of AI gum supported ZnO nanoparticles.

Conflict of Interest

The authors don't have any conflict of interest to disclose.

REFERENCES

1. Ikhmayies, S. *J. JOM.*, **2021**, *73*, 356–363. https://doi.org/10.1007/s11837-020-04495-9.
2. Payal Manzhi.; Reena Kumari.; Alam, Md. B.; Umapathy, G. R.; Richa Krishna.; Sunil Ojha.; Ritu Srivastava.; Sinha, O. P. *Vacuum.*, **2019,** *166*, 370-376. https://doi.org/10.1016/j.vacuum.2018.10.070.
3. Sharmin, A.; Tabassum,S.; Bashar, M. S.; Zahid Hasan Mahmood *J. Theor. Appl. Phys.*, **2019**, *13*, 123–132. https://doi.org/10.1007/s40094-019-0329-0.
4. Yanli Kang.; Feng Yu.; Lu Zhang.; Wenhao Wang.; Long Chen.; Yingchun Li. *Solid State Ion.*, **2021**, *360*, 115544. https://doi.org/10.1016/j.ssi.2020.115544.
5. Kamaci, U. D.; Kamaci, M. *J Fluoresc.*, **2021**, *31*, 401–414. https://doi.org/10.1007/s10895-020-02671-3.
6. Raj, R. B.; Umadevi, M.; Parimaladevi. R. *J Inorg Organomet Polym Mater.*, **2021**, *31*, 500–510. https://doi.org/10.1007/s10904-020-01717-0.
7. Pardeep Kumar.; Satya Dev.; Atul Kumar.; Rajesh Thakur.; Rakesh Dhar. *Superlattices Microstruct.*, **2021**, *150*, 06741. https://doi.org/10.1016/j.spmi.2020.106741.
8. Do Quang Trung.; Manh-Trung Tran.; Nguyen Duy Hung.; Quang Nguyen Van.; Nguyen Thi Huyen.; Nguyen Tu.; Huy Pham Thanh. *Opt. Mater.*, **2021**, *121*, 111587. https://doi.org/10.1016/j.optmat.2021.111587.
9. Aksay, S.; Aksoy Pehlivanoglu, S.; Hurma, T. *J. Mol. Struct.*, **2021**, *1225*, 129227. https://doi.org/10.1016/j.molstruc.2020.129227.
10. Anandh, BA.; Sakthivel, R.; Shankar Ganesh, A.; Subramani, S.; Rajamanickam, A.T. *Asian J. Chem.*, **2021**, *33*, 2393-2399. https://doi.org/10.14233/ajchem.2021.23342.
11. Jaballah, S.; Dahman, H.; Neri, G.; Mir, L. El. *J. Inorg Organomet Polym Mater.*, **2021**, *31*, 1653–1667. https://doi.org/10.1007/s10904-020-01796-z.
12. Al-Namshah, K. S.; Shkir, M.; Hamdy, M. S. *J Inorg Organomet Polym Mater.*, **2021**, *31*, 4338–4348. https://doi.org/10.1007/s10904-021-02049-3.

13. Nur Efsan Koksal.; Mohamed Sbeta.; Abdullah Atilgan.; Abdullah Yildiz. Physica B *Condens. Matter.*, **2021**, *600*, 412599. https://doi.org/10.1016/j.physb.2020.412599.

14. Lekoui, F.; Hassani, S.; Ouchabane, M.; Akkari, H.; Dergham, D.; Filali, W.; Garoudja, E. *Brazilian J. Phys.*, **2021**, *51*, 544–552. https://doi.org/10.1007/s13538-021-00866-y.

15. Ravichandran, A. T.; Karthick, R. *Results in Materials.*, **2020**, *5*, 100072.https://doi.org/10.1016/j.rinma.2020.100072.

16. Muhammad Shahid Nadeem.; Tauseef Munawar.; Faisal Mukhtar.; Muhammad Naveed-UR-Rahman.; Muhammad Riaz.; Faisal Iqbal. *Ceram. Int.*, **2021**, *47*, 11109-11121.https://doi.org/10.1016/j.ceramint.2020.12.234.

17. Shankar, D. B.; Bhagwat, V. R.; Shinde, A. B.; Jadhav, K.M. *Mater Sci Semicond Process.*, **2016**, *41*, 441-449. https://doi.org/10.1016/j.mssp.2015.10.002.

18. Bharati, V. A.; Sandeep, B. S.; Ashok, V. H.; Murumkar, V. D.; Sondur, V. V.; Jadhav, K. M. *J. Alloys Compd.*, **2020**, *821*, 153501. https://doi.org/10.1016/j.jallcom.2019.153501.

19. Mani, R.; Vivekanandan, K.; Vallalperuman, K. *J. Mater. Sci. Mater. Electron.*, **2017**, *28*, 4396–4402. https://doi.org/10.1007/s10854-016-6067-z.

20. Meera Ramachandra Gumaste.; Gururaj Anand Kulkarni. *Physica B Condens. Matter.*, **2021**, *615*, 413076. https://doi.org/10.1016/j.physb.2021.413076.

21. AlShammari, A. S.; Halim, M. M.; Yam, F. K.; Kaus, N. H. M. *Results Phys.*, **2020**, *19*, 103630.https://doi.org/10.1016/j.rinp.2020.103630.

22. Hasan, M. R.; Hamid, S. B. A.; Basirun, W. *J. Appl. Surf. Sci.*, **2015**, *339*, 22-27.https://doi.org/10.1016/j.apsusc.2015.02.162.

23. Huaming Mao.; Bin Zhang.; Yanli Nie.; Xiaoning Tang.; Sue Yang.; Shixin Zhou. *Appl. Surf. Sci.*, **2021**, *546*, 149127.https://doi.org/10.1016/j.apsusc.2021.149127.

24. Mohd Yusof, H.; Abdul Rahman, N.; Mohamad, R.; Hasanah Zaidan, U.; Samsudin, A. A. *Animals.*, **2021**, *11*, 2093.https://doi.org/10.3390/ani11072093.

25. Snega, S.; Ravichandran, K.; Baneto, M.; Vijayakumar, S. *J Mater Sci Technol.*, **2015**, *31*, 759-765. https://doi.org/10.1016/j.jmst.2015.03.001.

26. Ferin Fathima, A.; Jothi Mani, R.; Sakthipandi, K.; Manimala, K.; Aslam Hossain. *J. Inorg Organomet Polym Mater.*, **2020**, *30*, 2397–2405. https://doi.org/10.1007/s10904-019-01400-z.